Neurobiology of Aging 36 (2015) 680–692

Contents lists available at ScienceDirect

Neurobiology of Aging

journal homepage: www.elsevier.com/locate/neuaging

Aβ and NMDAR activation cause mitochondrial dysfunction involving ER calcium release

Ildete Luísa Ferreira [a,b], Elisabete Ferreiro [a,b], Jeannette Schmidt [a,b,c], João M. Cardoso [d], Cláudia M.F. Pereira [a,b,e], Ana Luísa Carvalho [a,b,f], Catarina R. Oliveira [a,b,e], A. Cristina Rego [a,b,e,*]

[a] Center for Neuroscience and Cell Biology (CNC), University of Coimbra, Coimbra, Portugal
[b] Institute for Interdisciplinary Research of the University of Coimbra (IIIUC), Coimbra, Portugal
[c] PhD Programme in Experimental Biology and Biomedicine (PDBEB), Center for Neuroscience and Cell Biology, University of Coimbra, Coimbra, Portugal
[d] Instrumentation Center, Physics Department, University of Coimbra, Coimbra, Portugal
[e] Faculty of Medicine, University of Coimbra, Coimbra, Portugal
[f] Department of Life Sciences, University of Coimbra, Coimbra, Portugal

ARTICLE INFO

Article history:
Received 6 November 2013
Received in revised form 26 August 2014
Accepted 2 September 2014
Available online 6 September 2014

Keywords:
Alzheimer's disease
Amyloid-β oligomers
Mitochondria
Calcium
N-methyl-D-aspartate receptor
GluN2B subunit

ABSTRACT

Early cognitive deficits in Alzheimer's disease (AD) seem to be correlated to dysregulation of glutamate receptors evoked by amyloid-beta (Aβ) peptide. Aβ interference with the activity of *N*-methyl-D-aspartate receptors (NMDARs) may be a relevant factor for Aβ-induced mitochondrial toxicity and neuronal dysfunction. To evaluate the role of mitochondria in NMDARs activation mediated by Aβ, we followed in situ single-cell simultaneous measurement of cytosolic free Ca^{2+} (Ca_i^{2+}) and mitochondrial membrane potential in primary cortical neurons. Our results show that direct exposure to Aβ + NMDA largely increased Ca_i^{2+} and induced immediate mitochondrial depolarization, compared with Aβ or NMDA alone. Mitochondrial depolarization induced by rotenone strongly inhibited the rise in Ca_i^{2+} evoked by Aβ or NMDA, suggesting that mitochondria control Ca^{2+} entry through NMDARs. However, incubation with rotenone did not preclude mitochondrial Ca^{2+} ($mitCa^{2+}$) retention in cells treated with Aβ. Aβ-induced Ca_i^{2+} and $mitCa^{2+}$ rise were inhibited by ifenprodil, an antagonist of GluN2B-containing NMDARs. Exposure to Aβ + NMDA further evoked a higher $mitCa^{2+}$ retention, which was ameliorated in GluN2B$^{-/-}$ cortical neurons, largely implicating the involvement of this NMDAR subunit. Moreover, pharmacologic inhibition of endoplasmic reticulum (ER) inositol-1,4,5-triphosphate receptor (IP_3R) and $mitCa^{2+}$ uniporter (MCU) evidenced that Aβ + NMDA-induced $mitCa^{2+}$ rise involves ER Ca^{2+} release through IP_3R and mitochondrial entry by the MCU. Altogether, data highlight $mitCa^{2+}$ dyshomeostasis and subsequent dysfunction as mechanisms relevant for early neuronal dysfunction in AD linked to Aβ-mediated GluN2B-composed NMDARs activation.

1. Introduction

Alzheimer's disease (AD) is the most common age-related neurodegenerative disease and the major cause of dementia in the elderly. Clinically, this disorder is characterized by global cognitive dysfunction, especially memory loss, and behavior and personality changes. The neuropathologic hallmarks of AD include extracellular deposits of amyloid-β (Aβ) peptide (produced after the metabolic processing of the amyloid precursor protein by β- and γ-secretases), intracellular neurofibrillary tangles (consisting of abnormally hyperphosphorylated tau protein), dystrophic neurites, and amyloid angiopathy. These histopathologic lesions were shown to be restricted to selective brain regions involved in memory and language, namely, the hippocampus and the cerebral cortex, which appear atrophic in AD patients (reviewed by Ferreira et al., 2010). Despite this, reduced dendritic spine density and synaptic integrity seem to better correlate with memory loss than histopathologic markers, which is consistent with the recognition of AD as a "synaptic disease." Indeed, studies in AD postmortem brain tissue samples and AD animal models support a role for disruption of

ILF and EF contributed equally for this study.

* Corresponding author at: Center for Neuroscience and Cell Biology (CNC), Faculty of Medicine, University of Coimbra, Rua Larga, 3004-504 Coimbra, Portugal. Tel.: +351 239 820190; fax: +351 239 822776.
E-mail address: a.cristina.rego@gmail.com (A.C. Rego).

0197-4580/$ – see front matter © 2015 Elsevier Inc. All rights reserved.
http://dx.doi.org/10.1016/j.neurobiolaging.2014.09.006

synaptic Ca^{2+} regulation in the neurotoxic action of Aβ (reviewed by Camandola and Mattson, 2011; Mota et al., 2014), which may serve as a trigger for synaptic deterioration driving the cognitive loss in AD. Interestingly, Aβ was shown to be produced in high amounts in synaptic terminals of the hippocampal dentate gyrus of transgenic mice and deposited in extracellular plaques (Lazarov et al., 2002). Thus, impaired cognitive function and memory loss observed in AD patients, associated to synaptic dysfunction, may be because of perturbed synaptic Ca^{2+} handling in response to overactivation of glutamate receptors, namely, the *N*-methyl-D-aspartate receptors (NMDARs) (Mota et al., 2014).

The most widely expressed NMDARs contain two obligatory GluN1 subunits plus GluN2B or GluN2A or a mixture of the two. NMDARs are concentrated on postsynaptic spines of neuronal dendrites being subjected to particularly high levels of Ca^{2+} influx, adenosine triphosphate (ATP) demand, and oxidative stress (Mattson et al., 1998). Concordantly, memantine, an uncompetitive antagonist of NMDARs, is used in AD patients and tested in several clinical trials as a neuroprotective and clinical stabilizer compound (http://www.clinicaltrials.gov), supporting the involvement of NMDARs on Aβ-induced neuronal damage. In accordance, NMDARs may be direct or indirect targets for Aβ, affecting the activity of these receptors (reviewed in Malinow, 2012). Aβ oligomers (5 μM) were reported to cause Ca^{2+} entry in neurons through NMDARs activation and consequent mitochondrial Ca^{2+} ($mitCa^{2+}$) overload (Alberdi et al., 2010; Sanz-Blasco et al., 2008). Indeed, during excitotoxicity, $mitCa^{2+}$ overload is one of the most important factors linked to mitochondrial dysfunction, occurring along with decreased mitochondrial membrane potential ($\Delta\Psi_m$) (e.g., Nicholls, 2009). We previously demonstrated that NMDARs activation leads to transient $mitCa^{2+}$ loading (e.g., Ward et al., 2000), which may be accompanied by oxidative damage to plasma membrane Ca^{2+} extrusion pathways and inhibition of mitochondrial respiration.

In AD postmortem brain and cellular and animal AD models, mitochondrial dysfunction can be triggered by Aβ (Pagani and Eckert, 2011). Interestingly, synaptic failure is strongly associated with synaptic mitochondrial dysfunction in AD, which occurs before changes in nonsynaptic mitochondria (for review, Dragicevic et al., 2010; Du et al., 2012). Studies in a transgenic mouse brain overexpressing the human mutant form of amyloid precursor protein and Aβ revealed that synaptic mitochondria undergo age-dependent accumulation of Aβ and mitochondrial alterations (Du et al., 2010). Aβ-induced mitochondrial dysfunction was reported to be related to the interaction of Aβ with different mitochondrial proteins, including proteins of the outer mitochondrial membrane, intermembrane space, inner mitochondrial membrane, and the matrix, impairing oxidative phosphorylation and mitochondrial dynamics and increasing reactive oxygen species (ROS) production (Pagani and Eckert, 2011). In this context, interaction of cyclophilin D (CypD, which is part of the mitochondrial permeability transition pore) with mitochondrial Aβ potentiated mitochondrial, neuronal, and synaptic stress; conversely, CypD-deficient cortical mitochondria were resistant to Aβ- and Ca^{2+}-induced mitochondrial swelling and permeability transition, along with increased calcium buffering capacity and production of fewer mitochondrial ROS (Du et al., 2008). More recently, genetic deletion of CypD suppressed Aβ-mediated activation of p38 mitogen-activated protein kinase signaling pathway, reversed axonal mitochondrial trafficking abnormalities, and improved synaptic function (Guo et al., 2013).

A high number of studies demonstrated the importance of NMDARs on Aβ toxicity, but the downstream interplay between endoplasmic reticulum (ER) and mitochondria is yet to be revealed. Recently, we observed the involvement of ER stress linked to nicotinamide adenine dinucleotide phosphate oxidase–mediated superoxide production in hippocampal neurons exposed to Aβ oligomers in a process involving the activation of NMDARs (Costa et al., 2012). To maintain normal cellular homeostasis, mitochondria and the ER directly communicate through the mitochondria-associated membranes (MAMs), which include inositol-1,4,5-triphosphate receptor (IP_3R) on the ER and the voltage-dependent anion channel in mitochondria (reviewed in Ferreiro et al., 2012). The Ca^{2+} released from ER, through IP_3R, can enter directly into mitochondria through the voltage-dependent anion channel in the outer mitochondrial membrane and through the $mitCa^{2+}$ uniporter (MCU) in the inner mitochondrial membrane. Dysfunction of these contact sites and $mitCa^{2+}$ overload can lead to the opening of permeability transition pore, dissipation of the $\Delta\Psi_m$, and activation of apoptotic cell death (Celsi et al., 2009). Interestingly, these receptors are involved in Aβ-induced release of Ca^{2+} from the ER, leading to depolarization of the mitochondrial membrane, release of cytochrome c on Bax translocation to mitochondria, and activation of apoptosis (Ferreiro et al., 2004, 2006, 2008). ER-mitochondria communication can thus play a fundamental role in AD pathogenesis.

Prolonged exposure to high concentrations of Aβ oligomers was shown to induce Ca^{2+} entry through NMDAR and AMPA receptors, mitochondrial dysfunction, and oxidative stress (Alberdi et al., 2010). More recently, we also demonstrated that immediate exposure to Aβ increases cytosolic free Ca^{2+} (Ca_i^{2+}) through the activation of NMDARs containing GluN2B subunits (Ferreira et al., 2012) and further demonstrated that Aβ can directly interact with the extracellular domain of GluN1 and GluN2B subunits and evoke ER stress downstream of GluN2B-composed NMDARs (Costa et al., 2012). Thus, the aim of this study was to evaluate the immediate effect of Aβ linked to NMDARs activation on mitochondrial function and the intricate role of mitochondria and ER interplay in Ca^{2+} homeostasis. Using in situ single-cell synchronized measurement of Ca_i^{2+} and $\Delta\Psi_m$ in rat primary brain cortical neurons, we show that simultaneous exposure to Aβ and NMDA affects the response to GluN2B-composed NMDARs, largely causing mitochondrial depolarization and $mitCa^{2+}$ retention. Moreover, $mitCa^{2+}$ accumulation via the MCU involved the release of ER Ca^{2+} through the IP_3Rs. These deleterious effects triggered by the simultaneous exposure to Aβ and activation of NMDARs may thus potentiate the neurodegenerative process in AD and contribute to cognitive impairment and dementia.

2. Methods

2.1. Primary neuronal cultures

2.1.1. Rat cortical cultures

Primary neuronal cultures of rat cerebral cortex were prepared as described previously (Agostinho and Oliveira, 2003) with some minor modifications. Briefly, frontal cerebral cortices were dissected from 16-day Wistar rat embryos and collected in Ca^{2+} Mg^{2+}-free Krebs medium containing (in millimolar) 120 NaCl, 4.33 KCl, 1.2 KH_2PO_4, 25.5 $NaHCO_3$, 13 glucose, 10 2-[4-(2-hydroxyethyl) piperazin-1-yl]ethanesulfonic acid (HEPES), pH 7.4, plus 0.3% (w/v) fatty acid–free bovine serum albumin (BSA). Tissues were treated with 0.035% (w/v) trypsin in BSA-Krebs medium, for 7 minutes at 37 °C, followed by addition of 0.038% (w/v) trypsin inhibitor and centrifugation at 140× *g* for 5 minutes. After a washing step, cells were resuspended in neurobasal medium (Gibco, Life Technologies, Paisley, UK) supplemented with 2% (v/v) B27 (Gibco), 0.5 mM glutamine, and 50 μg/mL gentamicin and plated in poly-D-lysine–coated glass coverslips, at a density of $0.2 \times 10^6/cm^2$. Cells were cultured for 8–9 days in vitro, in a humidified incubator chamber with 95% air and 5% CO_2 at 37 °C.

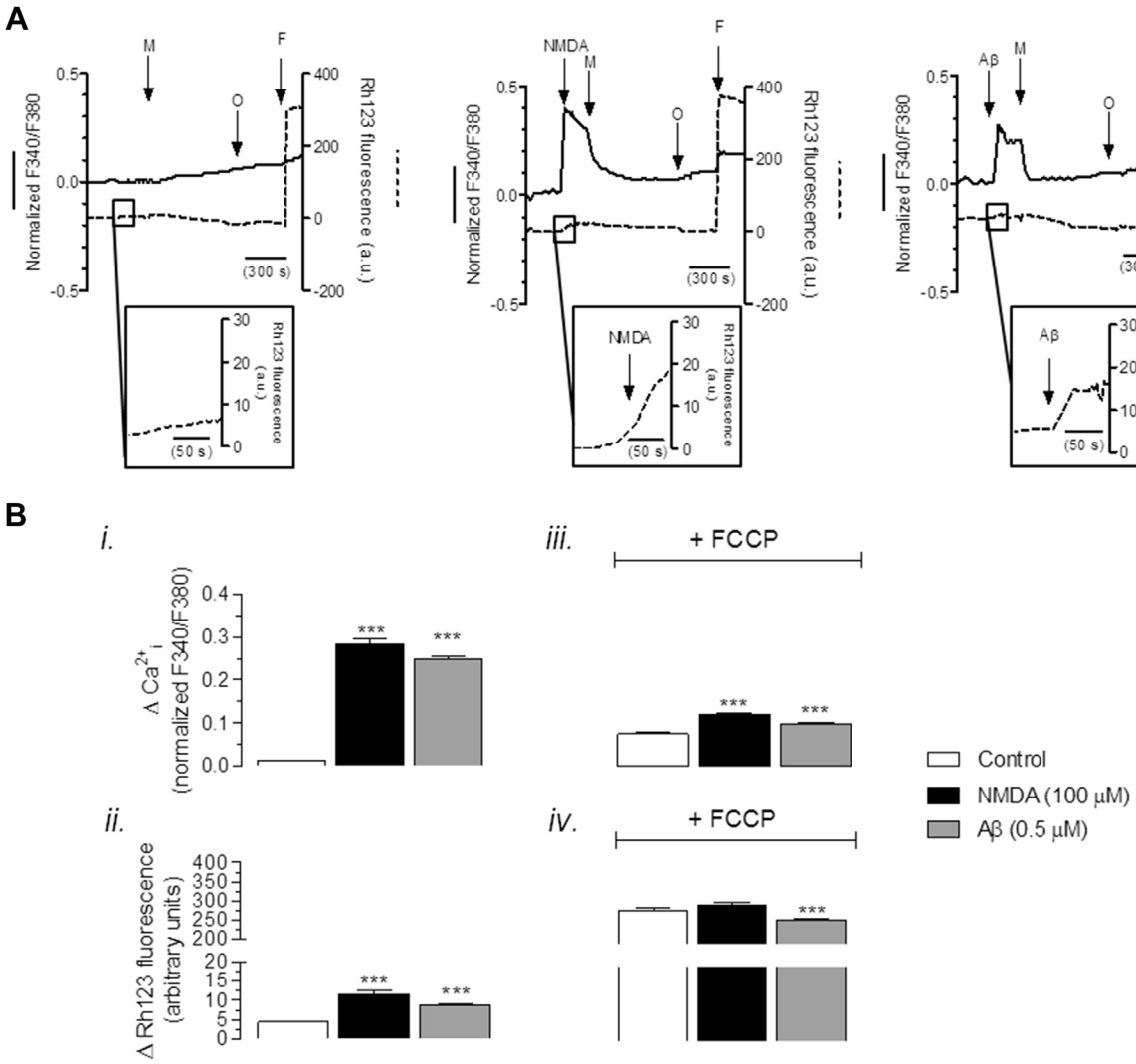

Fig. 1. *N*-methyl-D-aspartate (NMDA)–induced and amyloid-beta (Aβ)–induced changes in cytosolic free Ca^{2+} (Ca^{2+}_i) and mitochondrial membrane potential ($\Delta\Psi_m$). Cortical neurons were stimulated with NMDA (100 μM) or Aβ (0.5 μM). (A) Representative F340/F380 or rhodamine 123 (Rh123) fluorescence (arbitrary unit) traces from individual cells. (B) Peak amplitude of Fura-2 or Rh123 fluorescence after NMDA or Aβ, before and after FCCP (2 μM) exposure. Data are the mean ± standard error of the mean of 3–6 independent experiments, comprising a total of 163–270 cells per experimental group. Statistical analysis: $^{***}p < 0.001$ significantly different compared with the control (one-way analysis of variance with Bonferroni multiple comparison test). M, MK-801; F, FCCP; and O, oligomycin.

2.1.2. Mice cortical cultures from GluN2B$^{+/+}$ and GluN2B$^{-/-}$ embryos

Because GluN2B($^{-/-}$) mice die shortly after birth, GluN2B($^{+/-}$) mice (Kutsuwada et al., 1996) were mated to obtain GluN2B($^{-/-}$) and littermate control GluN2B$^{+/+}$ embryos, which were used to culture cortical neurons. Genotyping of pups and embryos was performed according to a previously described protocol (Tovar et al., 2000). Briefly, DNA was extracted with phenol/choloroform/isoamyl alcohol (Sigma, St Louis, MI, USA) after tissue digestion with proteinase K (0.1 mg/mL; Invitrogen, Life Technologies, Paisley, UK). polymerase chain reaction amplification using the Supreme NZYTaq 2× Green Master Mix (Nzytech, Lisboa, Portugal) was performed with specific primers for GluN2B (5′ ATG AAG CCC AGC GCA GAG TG 3′ and 5′ AGG ACT CAT CCT TAT CTG CCA TTA TCA TAG 3′) and for the neomycin cassette (5′ GGC TAC CTG CCC ATT CGA CCA CCA AGC GAA AC 3′). GluN2B$^{+/+}$ and GluN2B$^{-/-}$ cortical neuronal cultures were prepared from 17 to 18 days embryonic mice. Cortices were dissected and maintained in Hibernate E (Brain Bits, Springfield, IL, USA) supplemented with NeuroCult SM1 (Stemcell, Grenoble, France) at 4 °C overnight while genotyping was performed. Tissues from the same genotype were pooled together and dissociated with papain (20 units/mL, 10 minutes, 37 °C; Worthington Biochemical Corporation, Lakewood, NJ, USA) and deoxyribonuclease I (0.2 mg/mL, Invitrogen). Cortical neurons were plated at a density of 0.2 × 10^6/cm^2 on coverslips coated with poly-D-lysine in minimum essential medium supplemented with 10% horse serum. After ~3 hours in culture, the plating medium was replaced by neurobasal medium (Gibco) supplemented with 2% NeuroCult SM1, 0.5 mM glutamine (Sigma), 0.125 mg/mL gentamicin (Gibco), and insulin (20 μg/mL; Sigma). Neurons were maintained at 37 °C in a humidified incubator of 5% CO_2. Cultures were used after 8–9 days in vitro.

2.2. Experimental conditions

Experiments were performed in cells subjected to direct stimulation with 100-μM NMDA (Tocris, Bristol, UK) and/or 0.5 μM Aβ (American Peptide, Sunnyvale, CA, USA). Pre-exposure of cells to Aβ during 2 hours, before NMDA treatment, was also tested. $Aβ_{1–42}$ preparation containing ~60% of low *n* oligomers and ~40%

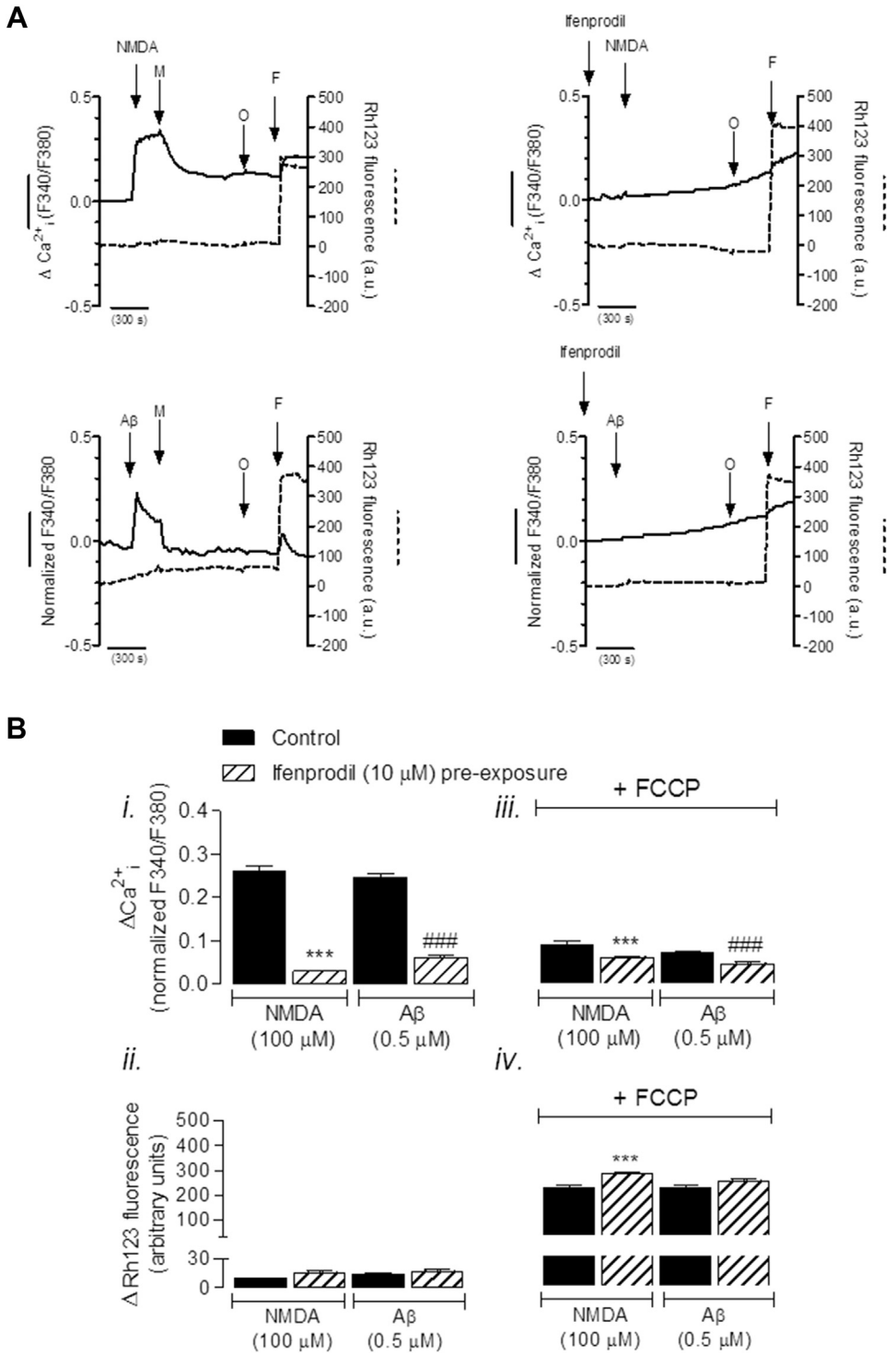

Fig. 2. Influence of ifenprodil on amyloid-beta (Aβ)–induced cytosolic free Ca^{2+} (Ca_i^{2+}) and mitochondrial membrane potential ($\Delta\Psi_m$). Cortical neurons were stimulated with *N*-methyl-D-aspartate (NMDA) (100 μM) or Aβ (0.5 μM) in the absence or presence of ifenprodil (selective GluN2B subunit antagonist, 10 μM). (A) Representative F340/F380 or rhodamine 123 (Rh123) fluorescence (arbitrary unit) traces from individual cells. (B) Peak amplitude of Fura-2 fluorescence after NMDA or Aβ stimulation in the absence or presence of ifenprodil, before and after FCCP (2 μM) exposure. For single-cell imaging studies, data are the mean ± standard error of the mean of 3–6 independent experiments, comprising a total of 118–230 cells per experimental group. Statistical analysis: $^{***}p < 0.001$ significantly different compared with NMDA; $^{\#\#\#}p < 0.001$ significantly different compared with Aβ (one-way analysis of variance with Bonferroni multiple comparison test). M, MK-801; F, FCCP; and O, oligomycin.

of monomers was obtained, as previously described (Ferreira et al., 2012). To assess the involvement of NMDARs in regulating Ca_i^{2+} homeostasis, cells were preincubated for 5 minutes with ifenprodil (10 μM; Sigma). To modulate mitochondrial function, cells were incubated for 3 minutes with 2 μM rotenone before the stimulation with NMDA and/or Aβ. To inhibit mitCa^{2+} accumulation and to evaluate the role of the MCU, cells were incubated with 10 μM ruthenium 360 (Ru360; Calbiochem, Darmstadt, Germany) during rhodamine 123 (Rh123) and Fura-2/AM loading and with fresh Ru360 during the experiment. To evaluate the contribution

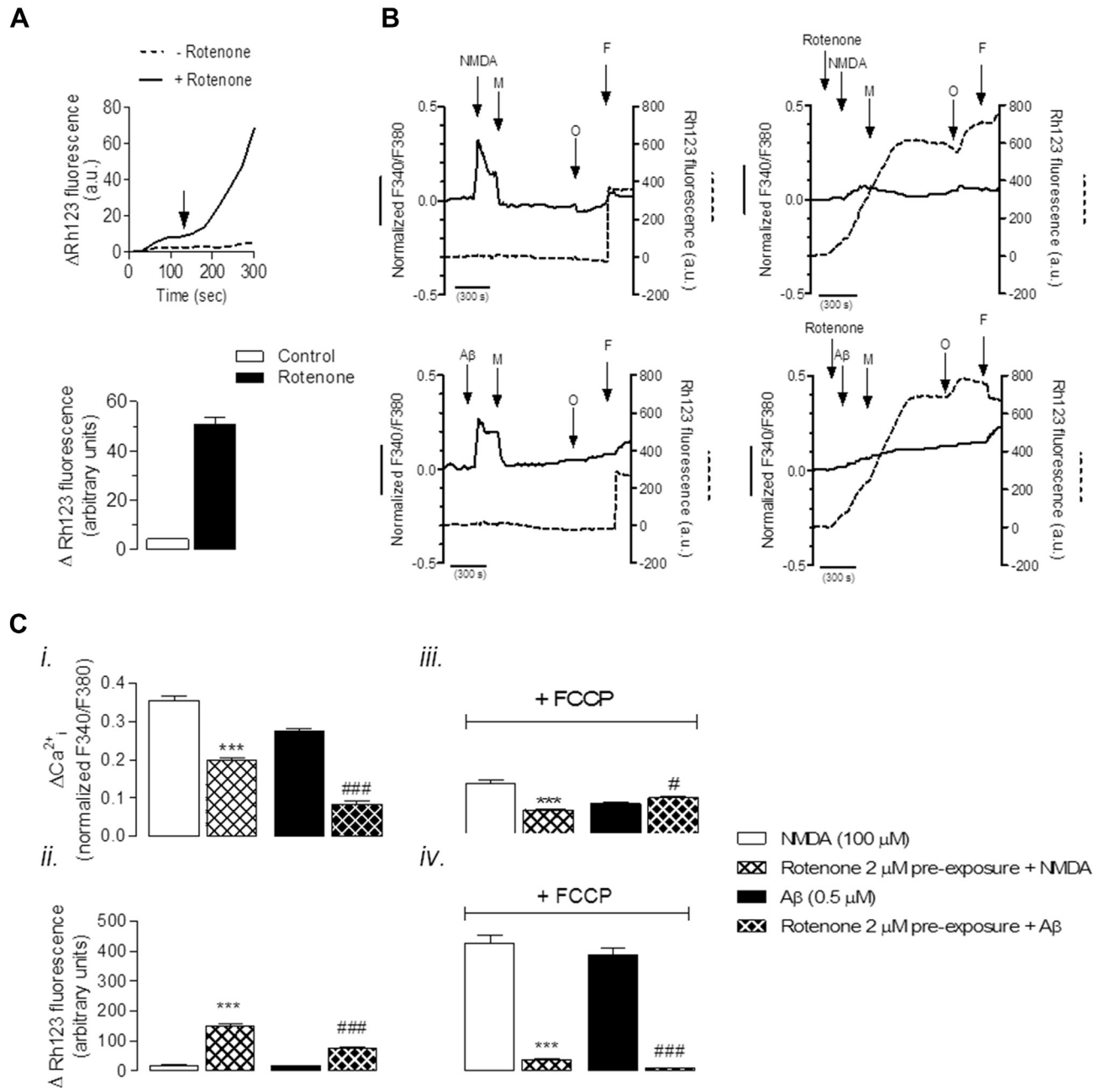

Fig. 3. Modulation of mitochondrial function by rotenone pre-exposure on *N*-methyl-D-aspartate (NMDA) or amyloid-beta (Aβ)–induced cytosolic free Ca^{2+} (Ca_i^{2+}) and mitochondrial membrane potential ($\Delta\Psi_m$). Cortical cells were stimulated with 0.5 μM Aβ or 100 μM NMDA in the absence or in the presence of rotenone (complex I inhibitor, 2 μM). (A) Magnification of the rotenone effect on $\Delta\Psi_m$. (B) Representative traces of Fura-2 or rhodamine 123 (Rh123) fluorescence after NMDA, Aβ, or rotenone pre-exposure. (C) Peak amplitude of Fura-2 and Rh123 fluorescence after NMDA or Aβ stimulation, before and after FCCP (2 μM) stimulation. Data are the mean ± standard error of the mean of 3–4 independent experiments, comprising a total of 123–199 cells per experimental group. Statistical analysis: $^{***}p < 0.001$ significantly different compared with NMDA alone, $^{\#}p < 0.05$ and $^{\#\#\#}p < 0.001$ significantly different compared with Aβ (one-way analysis of variance with Bonferroni multiple comparison test). M, MK-801; F, FCCP; and O, oligomycin.

of ER Ca^{2+} to the mitCa^{2+} content, cells were preincubated during 1 hour with 1 μM of xestospongin C (XeC; Tocris).

2.3. Monitoring dynamic changes in Ca_i^{2+} and $\Delta\Psi_m$

Cortical neurons, plated on glass coverslips, were washed with Na^+ medium containing (in millimolar) 140 NaCl, 5 KCl, 1 $CaCl_2$, 1 $MgCl_2$, 10 glucose, 10 HEPES, and pH 7.4/NaOH and loaded with Na^+ medium supplemented with the $\Delta\Psi_m$-sensitive probe (1.3 μM Rh123, quench mode) and 0.1% BSA for 10 minutes at room temperature. Then, glass coverslips were transferred to Na^+ medium containing 0.2% (w/v) pluoronic acid, 0.1% (w/v) BSA, 1.3 μM Rh123, and 5 μM Fura-2/AM for 30 minutes at 37 °C. The fluorescence probes Fura-2/AM and Rh123 were obtained from Molecular Probes, Life Technologies (Eugene, OR, USA). To directly assess the role of mitochondria, glycolysis was inhibited by adding 2-deoxy-D-glucose (2 mM) and by replacing glucose with pyruvate (10 mM) in Na^+ medium (pyruvate-based medium) (e.g., Oliveira et al., 2006; Rego et al., 2001). After rinsing with fresh buffer, coverslips were assembled in a nonperfused chamber filled with 500 μL of Mg^{2+}-free pyruvate medium containing 20 μM glycine, at room temperature. Simultaneous Ca_i^{2+} levels and Rh123 fluorescence were

measured by using an inverted fluorescence microscope Axiovert 200 (Zeiss, Jena, Germany) equipped with a dual-band path emission filter (510/40 and 600/60 nm) and a Lambda DG4 apparatus (Sutter Instruments Company, Novato, CA, USA). In situ calibration of Ca_i^{2+} responses was performed at the end of every individual experiment, by determining maximal 340/380 ratio for each individual cell, after the addition of 2 μM ionomycin (Sigma). Maximal mitochondrial depolarization ($\Delta\Psi_m$ collapse) was also performed in every individual experiment by adding a protonophore (2-μM carbonyl cyanide-4-(trifluoromethoxy)phenylhydrazone (FCCP); Sigma), which was preceded by oligomycin (2 μg/mL; Sigma) to prevent ATP synthase reversal. The determinations of fluorescence time courses were calculated on the basis of 1 microscopic field per coverslip, containing ~75 cells. Moreover, individual whole cells were identified as regions of interest.

2.4. Data analysis

Data analysis of single-cell imaging was performed with systematic custom scripts of Mathworks Matlab 2007a (32 bits) for fluorescence time-course parametrization. For each experiment condition, a cell response normalization procedure to the time-course basal level (first value obtained) was performed. The peak from the first stimulus amplitude histogram of Fura-2 (340/380 ratios) time course was used to interactively set a cut-off level, adjusted for each experiment, to remove low-amplitude time courses from nonresponsive cells. Therefore, only data from responsive cells were considered for peak amplitude measurements. These were performed by means of the highest 340/380 ratio difference in the vicinity of the registered peak in analysis. Notice that the cut-off exclusion criteria were not applied in the experiments involving rotenone and ifenprodil pre-exposure. Each experimental condition was assayed at least in three different coverslips from three independent culture preparations.

Data were expressed as mean ± standard error of the mean of the number of experiments indicated in Figs. 1–6. Comparisons among multiple groups were performed by one- or two-way analysis of variance, followed by Bonferroni post hoc test or Student *t* test, as described in the figure legends. Significance was accepted at $p < 0.05$.

3. Results

In this work, we detailed the single-cell simultaneous changes in Ca_i^{2+} and $\Delta\Psi_m$ in brain cortical cells stimulated with NMDA (100 μM), Aβ (0.5 μM), simultaneous exposure to Aβ plus NMDA (Aβ + NMDA), or incubation with NMDA in cells pre-exposed for 2 hours to Aβ. These changes were followed in basal conditions or after maximal mitochondrial depolarization achieved by the mitochondrial uncoupler FCCP in conditions of ATP synthase inhibition, in the presence of oligomycin, to prevent ATP hydrolysis.

3.1. Aβ induces immediate Ca_i^{2+} rise and depolarization of mitochondrial membrane

Our results show that NMDA and, to a less extent, Aβ cause a robust increase in Ca_i^{2+} levels (Fig. 1A and B*i*) associated with a slight decrease in $\Delta\Psi_m$ (Fig. 1B*ii*), compared with the maximum depolarization obtained with FCCP (see representative traces in Fig. 1A). Complete mitochondrial depolarization induced by FCCP in cells treated with NMDA increased Rh123 fluorescence comparable with the control, indicating unaltered $\Delta\Psi_m$ ~20 minutes after the initial stimuli; Aβ-treated cells showed reduced mitochondrial accumulation of Rh123 after incubation with FCCP, indicating decreased $\Delta\Psi_m$ (Fig. 1A and B*iv*). Importantly, the higher increase in Ca_i^{2+} levels achieved by NMDA and Aβ was associated with an increase in $mitCa^{2+}$, as represented by the rise in mitochondrial FCCP-releasable Ca^{2+} pool (Fig. 1A and B*iii*). Our results show that immediate stimulation of cortical cells with Aβ induces a significant increase in Ca_i^{2+} levels and mitochondrial membrane depolarization, associated with $mitCa^{2+}$ retention.

3.2. Aβ-induced Ca_i^{2+} rise and mitochondrial depolarization are prevented by selective blockade of GluN2B subunits

To characterize the involvement of NMDARs, in particular the GluN2B subunit, in Ca_i^{2+} changes evoked by NMDA or Aβ, as previously demonstrated by us (Costa et al., 2012; Ferreira et al., 2012), cells were stimulated with NMDA or Aβ in the absence or presence of the selective GluN2B subunit antagonist ifenprodil (Fig. 2). Our results demonstrate that Ca_i^{2+} increase exerted by NMDA or Aβ was significantly counteracted by ifenprodil (Fig. 2A and B*i*). Interestingly, the disruption of $\Delta\Psi_m$ induced by NMDA and Aβ was not affected by the NMDARs antagonist (Fig. 2A and B*ii*). Moreover, the increase in $mitCa^{2+}$ retention elicited by NMDA and by Aβ was also partially decreased (approximately by half) in the presence of ifenprodil (Fig. 2A and B*iii*). These data show a fundamental role of GluN2B subunits in defining Aβ-evoked Ca_i^{2+} rise and $mitCa^{2+}$ accumulation. Maximal Rh123 cytosolic release achieved by oligomycin plus FCCP in cells exposed to NMDA was shown to be slightly increased in the presence of ifenprodil (Fig. 2A and B*iv*), suggesting a rise in $\Delta\Psi_m$.

3.3. Rotenone-induced mitochondrial depolarization modulates Aβ-induced changes in Ca_i^{2+} and $\Delta\Psi_m$

To evaluate the contribution of functional mitochondria in controlling Ca_i^{2+} levels, cells were incubated for 3 minutes with 2 μM rotenone (complex I inhibitor and depolarizing agent) before stimulation with NMDA or Aβ. These were added under conditions of mild depolarization evoked by rotenone, that is, before complete rotenone depolarization (that was achieved after ~15 minutes incubation), to detect synergistic effects of NMDA or Aβ. Results depicted in Fig. 3A demonstrate that rotenone *per se* induced a significant decrease in $\Delta\Psi_m$, as observed by the large increase in Rh123 fluorescence. Moreover, mitochondrial dysfunction induced by rotenone attenuated the rise in Ca_i^{2+} induced by immediate exposure to NMDA or Aβ (Fig. 3B and C*i*) and enhanced mitochondrial depolarization in response to NMDA and Aβ stimulation (Fig. 3B and C*ii*). Complete mitochondrial depolarization, achieved by oligomycin plus FCCP in cells preincubated with rotenone, evidenced a decrease in $mitCa^{2+}$ retention in cells exposed to NMDA. Conversely, a very slight but significant increase in $mitCa^{2+}$ retention was observed in Aβ-treated cells pre-exposed to rotenone (Fig. 3B and C*iii*), which may suggest that Aβ-evoked $mitCa^{2+}$ retention is not primarily dependent on the maintenance of $\Delta\Psi_m$. Moreover, oligomycin-evoked mitochondrial depolarization was observed in cells treated with rotenone (Fig. 3B), indicative of mitochondrial ATP hydrolysis (e.g., Ward et al., 2000). Despite this, and as expected, exposure to FCCP evidenced a complete mitochondrial depolarization (Fig. 3B and C*iv*).

These results suggest that mitochondrial function modulates Ca_i^{2+} rise after exposure to NMDA and Aβ. In contrast with NMDA, Aβ-evoked $mitCa^{2+}$ accumulation does not seem to be accounted for by preserved mitochondrial function.

3.4. Increased $mitCa^{2+}$ accumulation and decreased $\Delta\Psi_m$ after exposure to Aβ + NMDA

Impairment in glutamatergic neurotransmission has been suggested to occur concomitantly with the presence of extracellular

levels of Aβ oligomers (Parameshwaran et al., 2008). Thus, the effect of simultaneous addition of NMDA and Aβ or NMDA in cells pre-exposed to Aβ for 2 hours was then evaluated. Interestingly, Aβ + NMDA stimulation produced a significant rise in Ca_i^{2+} levels, compared with NMDA or Aβ alone (Fig. 4B and C*i*), and preincubation with Aβ for 2 hours significantly decreased Ca_i^{2+} levels in response to NMDA stimulation, compared with cells not previously exposed to Aβ (Fig. 4B and C*i*). Both pre- and simultaneous exposure to Aβ affected the response to NMDAR activation, largely causing an additional immediate mitochondrial depolarization, compared with Aβ or NMDA alone (Fig. 4B and C*ii*). Notably, mitCa^{2+} retention capacity was largely increased on addition of Aβ + NMDA, compared with NMDA or Aβ alone, or even after NMDA stimulation in cells pre-exposed to Aβ (Fig. 4B and C*iii*). Moreover, cortical cultures treated with Aβ + NMDA or NMDA on pre-exposure to Aβ showed reduced retention of Rh123, compared with NMDA or Aβ alone, evidencing increased mitochondrial depolarization (Fig. 4B and C*iv*).

These data suggest the activation of different cellular mechanisms after addition of Aβ + NMDA, compared with previous exposure with Aβ followed by NMDA exposure. Indeed, incubation for 2 hours with Aβ *per se* caused a slight but significant rise in Ca_i^{2+} and mitochondrial depolarization, in comparison with untreated conditions (Fig. 4A).

3.5. Decreased Ca_i^{2+} rise and mitochondrial depolarization in GluN2B($^{-/-}$) cortical neurons

To confirm the involvement of the GluN2B subunit in both Ca_i^{2+} levels and mitochondrial membrane potential, we tested cortical cultures derived from GluN2B($^{-/-}$) mice treated with NMDA, Aβ, and Aβ + NMDA (Fig. 5). Our results demonstrated that Ca_i^{2+} increase exerted by the 3 stimuli was significantly reduced in GluN2B($^{-/-}$) cortical cultures, compared with GluN2B$^{+/+}$ cells (Fig. 5A and B*i*) and closely associated with lower mitochondrial depolarization (Fig. 5A and B*ii*). The extent of Ca_i^{2+} rise and mitochondrial depolarization was higher after exposure to Aβ + NMDA (as verified in Fig. 4C*i* and *ii*), compared with NMDA or Aβ stimulation alone. Interestingly, mitCa^{2+} content was significantly higher in GluN2B($^{-/-}$) compared with GluN2B$^{+/+}$ cells, in the absence (control) or presence of NMDA (Fig. 5A and B*iii*). Exposure to Aβ + NMDA in GluN2B$^{+/+}$ cells was associated with increased mitCa^{2+} (Fig. 5B*iii*), similarly as observed in rat cortical cells (Fig. 4C*iii*). However, exposure to Aβ or Aβ + NMDA in cells from GluN2B($^{-/-}$) mice largely reduced the capacity of mitochondria to retain Ca^{2+} (Fig. 5B*iii*). This lower mitCa^{2+} retention after Aβ exposure was linked to increased mitochondrial membrane potential in GluN2B($^{-/-}$)–derived cells (Fig. 5A and B*iv*), confirming an important role of this NMDAR subunit in facilitating mitCa^{2+} accumulation and the consequent mitochondrial depolarization.

3.6. Increased mitCa^{2+} accumulation induced by Aβ + NMDA is modulated by IP_3R and MCU

Previous studies showed that Aβ activates the IP_3-generating phospholipase C and triggers ER Ca^{2+} release via IP_3R-sensitive channels (Resende et al., 2008) and that ER-to-mitochondria Ca^{2+} transfer is involved in neuronal dysfunction induced by Aβ (Ferreiro et al., 2008). To clarify the mechanism involved in enhanced mitCa^{2+} retention that occurs in cells exposed to Aβ + NMDA (Fig. 4C*iii*), both Ca_i^{2+} entry and the IP_3R-mediated transfer of Ca^{2+} from the ER to mitochondria were evaluated and compared with Aβ treatment. For this purpose, cortical cells were preincubated with Ru360, an MCU inhibitor, or with XeC, an inhibitor of the IP_3R (Fig. 6).

Our results demonstrate that inhibition of Ca^{2+} release through the IP_3R significantly attenuated the increase in Ca_i^{2+} levels (Fig. 6*i*) and reduced mitochondrial depolarization (Fig. 6*i*) evoked by simultaneous exposure to Aβ + NMDA (as shown in Fig. 4B and 4C*i* and *ii*). Importantly, a reduction in mitochondria Ca^{2+} retention was observed when the cells were pre-exposed to Ru360 and treated with Aβ + NMDA (Fig. 6*ii*), suggesting that under this experimental condition, MCU contributes for mitCa^{2+} retention. In these cells, a significant decrease in Ca^{2+} uptake by mitochondria (Fig. 6*iii*) and a rescue in mitochondrial membrane potential (Fig. 6*iv*) were also observed when the release of Ca^{2+} through IP_3R was blocked. These data demonstrate that simultaneous exposure to Aβ + NMDA causes the release of Ca^{2+} through IP_3R and the entry to mitochondria through the MCU.

4. Discussion

The present study uncovers a fundamental mechanism underlying Aβ-induced synaptic dysfunction, namely, the link between NMDARs activation and mitochondrial dysregulation, particularly their capacity to handle Ca^{2+} in cultured cortical neurons. By using in situ single-cell simultaneous measurement of Ca_i^{2+} levels and $\Delta\Psi_m$, we show that cells challenged simultaneously with Aβ oligomeric–enriched preparation, the main synaptotoxic species involved in AD (Haass and Selkoe, 2007; Klein, 2006) and to the NMDARs agonist NMDA exhibit elevated Ca_i^{2+} levels, leading to mitCa^{2+} retention and depolarization through a pathway that involves both ER IP_3R and the MCU. The data evidence the dynamics between NMDARs activity and ER-mitochondria interplay in Ca^{2+} homeostasis and the resulting mitochondrial (dys)function in response to an immediate effect of Aβ.

Sustained changes in Ca^{2+} homeostasis that occur during aging were earlier described to be in the origin of the development of neurodegenerative diseases (Gibson and Peterson, 1987), namely AD. Importantly, NMDARs dysregulation evoked by Aβ and the consequent loss of Ca^{2+} homeostasis are thought to be related to the early cognitive deficits observed in this disorder. Several mechanisms have been suggested for Aβ-mediated Ca_i^{2+} rise, namely: (1) formation of Aβ Ca^{2+}-permeable pores in the plasma membrane (Arispe et al., 1993); (2) activation of pre-existing ion channels, which include the NMDARs (De Felice et al., 2007; Ferreira et al., 2012); and/or (3) induction of Ca^{2+} release from internal stores (Ferreiro et al., 2008; Resende et al., 2008; reviewed in Supnet and Bezprozvanny, 2010). By either being a direct or indirect target of Aβ, NMDARs play a fundamental role in Aβ toxicity (reviewed in Malinow, 2012). Aβ was reported to bind to or be in close proximity to NMDARs, triggering neuronal damage through NMDARs-dependent Ca^{2+} influx (Costa et al., 2012; De Felice et al., 2007). Indeed, we demonstrated that, in rat hippocampal neurons, blockade of extracellular domains of GluN1 or GluN2B, but not GluN2A, subunits reduces the binding of Aβ oligomers (Costa et al., 2012). Conversely, Aβ-induced activation of GluN2A-containing NMDARs in non-neuronal cells, namely in *Xenopus laevis* oocytes (Texidó et al., 2011) and HEK293cells (Domingues et al., 2007), was previously reported. In the AD brain and human cortical neurons, excitatory synapses containing the GluN2B subunit of the NMDARs appear to be the main sites of oligomer accumulation (Deshpande et al., 2009). Recently, we showed that Aβ increased Ca_i^{2+} levels through the activation of NMDARs containing GluN2B subunits, shown to be present at the membrane surface in cortical neurons (Ferreira et al., 2012), which may result in microtubule disassembly and reduced neurite length (Mota et al., 2012). One possible destination for Ca^{2+} that enters through the NMDARs are the Ca^{2+} internal stores, namely, the mitochondria and the ER. Recently, we showed that Aβ triggers ER stress by an NMDARs-dependent mechanism, leading to neuronal dysfunction (Costa et al., 2012).

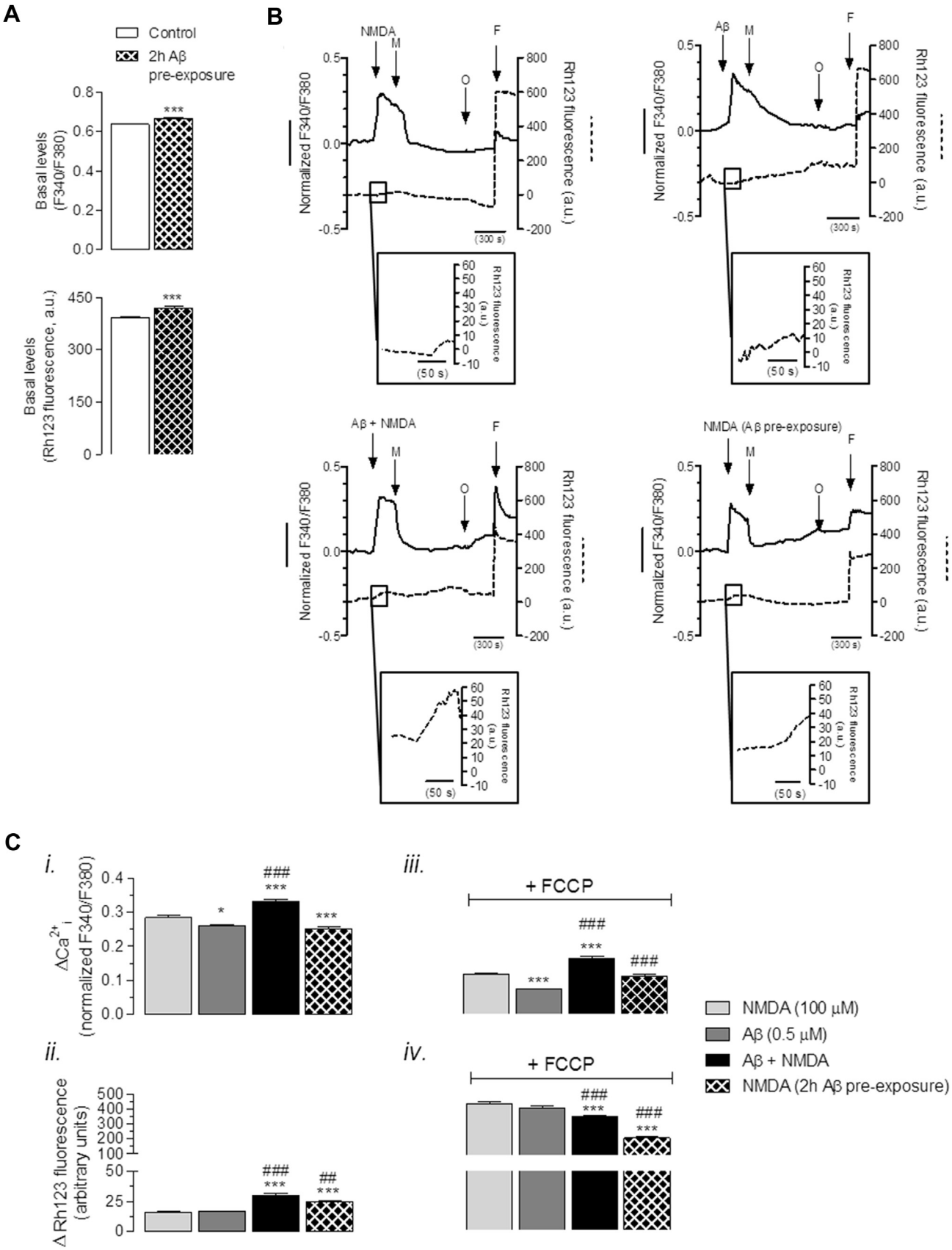

Fig. 4. Single-cell analysis of free cytosolic Ca^{2+} (Ca_i^{2+}) and mitochondrial membrane potential ($\Delta\Psi_m$) on *N*-methyl-D-aspartate (NMDA), amyloid-beta (Aβ), Aβ + NMDA stimulation or NMDA in cells pre-exposed to Aβ. Cortical cells were stimulated with 100 μM NMDA, 0.5 μM Aβ, Aβ + NMDA, or NMDA in cells pre-exposed for 2 hours to Aβ. (A) Basal levels of Fura-2 or rhodamine 123 (Rh123) fluorescence after 2 hours of exposure to Aβ. (B) Representative F340/F380 or Rh123 fluorescence (arbitrary unit) traces from individual cells.

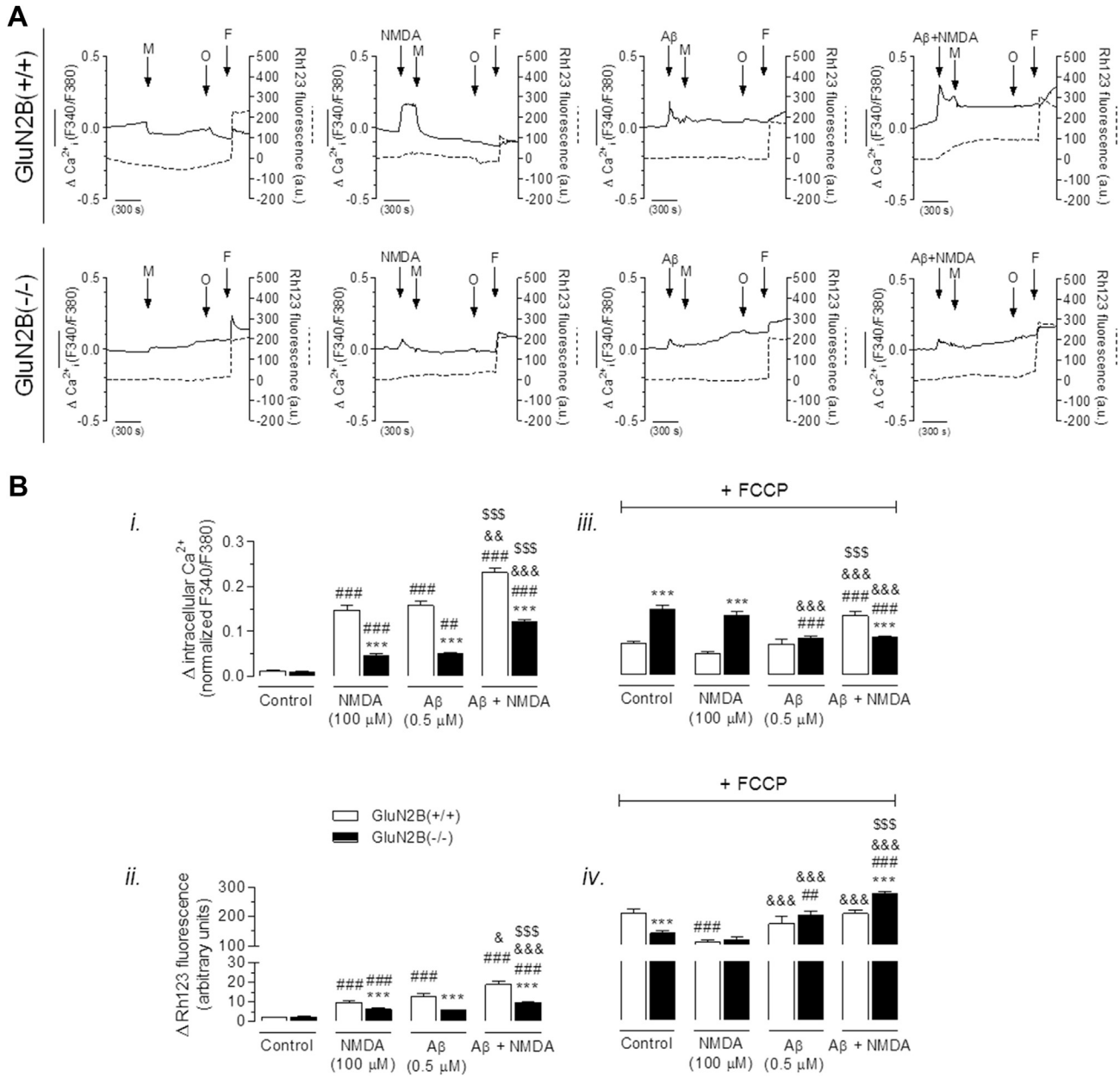

Fig. 5. Role of GluN2B subunits on single-cell analysis of Ca_i^{2+} and mitochondrial membrane potential ($\Delta\Psi_m$). GluN2B$^{-/-}$ versus GluN2B$^{+/+}$ mouse cortical neurons were stimulated with 100 μM *N*-methyl-D-aspartate (NMDA), 0.5 μM amyloid-beta (Aβ), or Aβ + NMDA. (A) Representative F340/F380 or rhodamine 123 (Rh123) fluorescence (arbitrary unit) traces from individual cells. (B) Peak amplitude of Fura-2 or Rh123 fluorescence after NMDA, Aβ, or Aβ + NMDA stimulation before or after FCCP (2 μM) stimulation. Data are the mean ± standard error of the mean of 3–4 independent experiments, comprising a total of 69–358 cells per experimental group. Statistical analysis: $^{***}p < 0.001$ when GluN2B$^{-/-}$ cells are compared with GluN2B$^{+/+}$ cells; $^{\#\#}p < 0.01$ and $^{\#\#\#}p < 0.001$ compared with control conditions; $^{\&}p < 0.05$, $^{\&\&}p < 0.01$, and $^{\&\&\&}p < 0.001$ compared with NMDA alone; and $^{\$\$\$}p < 0.001$ compared with Aβ alone (two-way analysis of variance with Bonferroni multiple comparison test). M, MK-801; F, FCCP; and O, oligomycin.

The present results demonstrate that Aβ preparation enriched in oligomeric forms induces Ca_i^{2+} rise and immediate mitochondrial depolarization, similarly to the selective activation of NMDARs with NMDA and that part of Ca_i^{2+} is further accumulated within mitochondria. Our experiments were performed in the presence of glycine, which favors the activation of extrasynaptic GluN2B-containing NMDARs. These observations are in accordance with the findings in the CA1 region of the hippocampus demonstrating that synaptic and extrasynaptic NMDARs are gated by different endogenous co-agonists, respectively, D-serine and glycine (Papouin et al., 2012). We confirmed that Ca_i^{2+} changes were largely mediated by GluN2B subunits because both Ca_i^{2+} and mitCa^{2+} accumulation were prevented by ifenprodil, a selective inhibitor of GluN2B-containing NMDARs. This inhibition of Ca^{2+} entry through NMDARs did not affect $\Delta\Psi_m$ as determined immediately after the NMDA or Aβ stimuli and slightly induced mitochondrial Rh123

(C) Peak amplitude of Fura-2 or Rh123 fluorescence after NMDA, Aβ, Aβ + NMDA stimulation or NMDA in cells pre-exposed for 2 hours to Aβ, before or after FCCP (2 μM) stimulation. Data are the mean ± standard error of the mean of 10–15 independent experiments, comprising a total of 591–676 cells per experimental group. Statistical analysis: $^{*}p < 0.05$, $^{***}p < 0.001$ significantly different compared with the control (A, by Student *t* test) or NMDA exposure (C); $^{\#\#}p < 0.01$, $^{\#\#\#}p < 0.001$ significantly different compared with Aβ (one-way analysis of variance with Bonferroni multiple comparison test). M, MK-801; F, FCCP; and O, oligomycin.

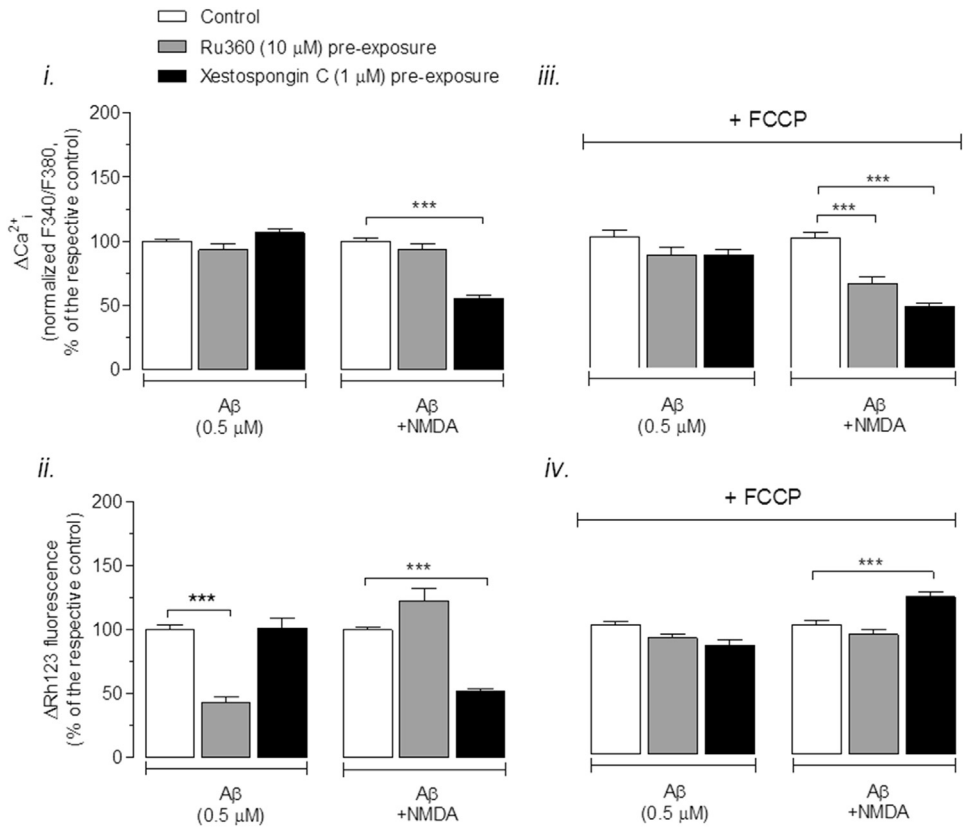

Fig. 6. Modulation by inositol-1,4,5-triphosphate receptor (IP_3R) and mitochondrial Ca^{2+} uniporter of Ca_i^{2+} and mitochondrial membrane potential ($\Delta\Psi_m$) after exposure to amyloid-beta (Aβ) or Aβ + *N*-methyl-D-aspartate (NMDA). Cortical cells were stimulated with 0.5 μM Aβ or Aβ + NMDA in the absence or presence of Ru360 ($mitCa^{2+}$ uniporter inhibitor, 10 μM) or xestospongin C (XeC) (IP_3R inhibitor, 1 μM). The results are expressed as the percentage of the respective control (Aβ or Aβ + NMDA), in the absence of the inhibitors; data are the mean ± standard error of the mean of 3–5 independent experiments, comprising a total of 115–366 cells per experimental group. Statistical analysis: $^{***}p < 0.001$ significantly different compared with the respective control (one-way analysis of variance with Bonferroni multiple comparison test).

retention (as shown in NMDA-treated cells), suggesting that the observed decrease in NMDARs-coupled Ca^{2+} entry is not sufficient for largely modifying the $\Delta\Psi_m$ in cultured neurons. However, the close relationship between mitochondrial function and NMDARs activation is evident in rotenone-treated cells. Thus, our data suggest that Aβ-induced Ca_i^{2+} dyshomeostasis is, at least in part, because of excessive activation of NMDARs composed by GluN2B subunits.

Excitotoxicity is normally precluded by astrocytic glutamate transporters, an event that is counteracted by Aβ because of the downregulation of the astrocytic glutamate uptake capacity (Matos et al., 2008). Concomitantly with AD progression, an imbalance in glutamatergic neurotransmission, because of the increase in glutamate levels at the synaptic cleft, may occur along with extracellular Aβ oligomer accumulation, which may potentially exacerbate NMDARs activation and promote Ca_i^{2+} dyshomeostasis. Our previous work demonstrated that simultaneous addition of Aβ + NMDA leads to a large increase in Ca_i^{2+} levels compared with the effect of NMDA or Aβ alone and that this effect is prevented by GluN2B-containing NMDARs (Ferreira et al., 2012). The present study further demonstrates that enhanced $mitCa^{2+}$ evoked by Aβ + NMDA is partially precluded in $GluN2B^{-/-}$ cortical neurons, implicating this NMDAR subunit in facilitating $mitCa^{2+}$ accumulation and the consequent mitochondrial depolarization. Moreover, sustained incubation (for 2 hours) with Aβ induced a slight but significant decrease in Ca_i^{2+} levels evoked by further stimulation with NMDA, along with a significant increase in mitochondrial depolarization, compared with that occurring in response to NMDA alone. Although NMDA stimulation in cells subjected to Aβ pre-exposure induced similar levels of $mitCa^{2+}$ retention, resembling those obtained with NMDA alone, mitochondria were largely depolarized, which may be accounted for by the prolonged pre-exposure to Aβ. This indicates that mitochondrial depolarization occurred during Aβ exposure (before incubation with NMDA), impairing Ca_i^{2+} increase, which appears to be in accordance with the effect of rotenone on NMDARs modulation. Exposure for 2 hours with high concentration of $Aβ_{1–42}$ oligomers (5 μM) was previously shown to cause mitochondrial depolarization and oxidative stress, dependent on the activation of NMDA and AMPA receptors (Alberdi et al., 2010).

Interestingly, in the present work, we show that Aβ and NMDA co-stimulation elevate Ca_i^{2+} levels and that this increase in Ca^{2+} is associated with enhanced $mitCa^{2+}$ retention and mitochondrial depolarization. In accordance with our data, inhibiting $mitCa^{2+}$ clearance accelerated mitochondrial depolarization (Stanika et al., 2012). Indeed, $mitCa^{2+}$ overload, along with mitochondrial depolarization ($\Delta\Psi_m$ dissipation), is strongly linked to mitochondrial dysfunction (e.g., Nicholls, 2009), reinforcing mitochondria as a target of Aβ in AD pathology (for review, Pagani and Eckert, 2011). Intraneuronal Aβ accumulation occurs early in the neuropathologic phenotype of AD, before neurofibrillary tangle formation and plaque deposition (Gouras et al., 2000). Intracellular Aβ was suggested to occur because of internalization of extracellular Aβ after the interaction of presecreted Aβ with membrane transporters and receptors, including α-7 nicotinic acetylcholine receptors, advanced glycation end products receptors, and NMDARs (reviewed by Caldeira et al., 2013). Aβ uptake was completely blocked by NMDAR antagonists, evidencing an involvement of this receptor in the re-uptake of the peptide (Bi et al., 2002). Moreover, it was previously demonstrated that Aβ is

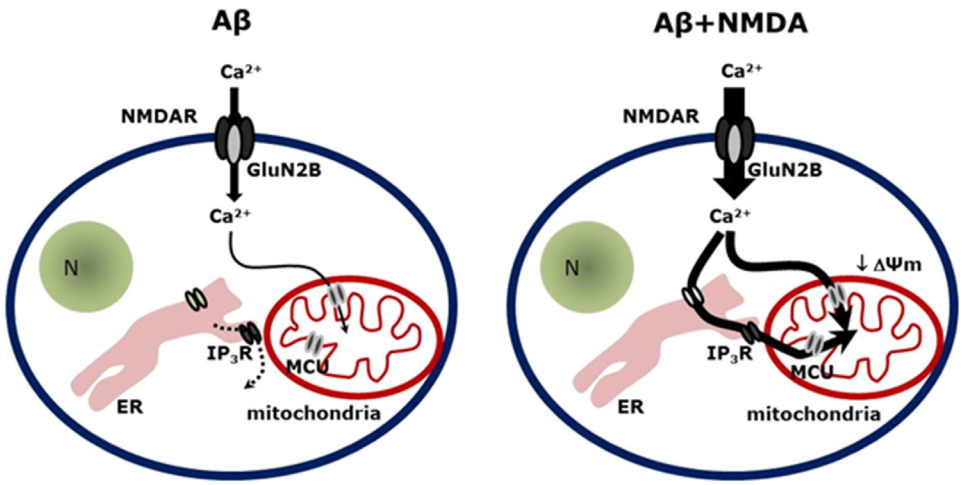

Fig. 7. Proposed molecular pathways for amyloid-beta (Aβ) or Aβ + *N*-methyl-D-aspartate (NMDA) modulation of Ca_i^{2+} and mitochondrial membrane potential ($\Delta\Psi_m$). Aβ induces an increase in Ca_i^{2+} and an immediate mitochondrial depolarization in cortical neurons, mediated by GluN2B-containing NMDA receptor (NMDAR) activation. Ca^{2+} entry through NMDAR is taken up by the endoplasmic reticulum (Costa et al., 2012), which may be released by the inositol-1,4,5-triphosphate receptor (IP_3R) (Resende et al., 2008). After exposure to Aβ + NMDA, Ca_i^{2+} increase is potentiated, inducing mitochondrial depolarization and enhanced mitochondrial Ca^{2+} retention through a pathway that involves the release of Ca^{2+} through IP_3R and the entry to the mitochondria by the $mitCa^{2+}$ uniporter. (For interpretation of the references to color in this figure, the reader is referred to the web version of this article.)

transported into mitochondria via the translocase of the outer membrane machinery and is located in mitochondria cristae (Hansson Petersen et al., 2008). Aβ interferes with oxidative phosphorylation and ROS production within mitochondria and causes decreased $\Delta\Psi_m$, complex IV (cytochrome c oxidase) activity, and ATP production (Hauptmann et al., 2009). By using isolated rat brain mitochondria treated with Aβ, both mitochondrial transmembrane potential and the mitochondrial capacity to accumulate Ca^{2+} were shown to be decreased and to cause complete uncoupling of respiration (Moreira et al., 2001). More recently, hippocampal and cortical mitochondria of cognitive impaired AD transgenic mice showed high levels of dysfunction, whereas striatal and amygdala mitochondria were less affected (Dragicevic et al., 2010), reinforcing increased mitochondrial dysfunction in selective brain areas mostly affected in AD. In addition, transcription regulators related with mitochondrial biogenesis and antioxidant defenses are altered in different AD models (reviewed by Caldeira et al., 2013), implicating mitochondrial dysfunction in AD.

In our model, rotenone-induced high mitochondrial depolarization reduced Ca_i^{2+} increase promoted by Aβ or NMDA, implicating the fundamental role of functional mitochondria in the activity of ionotropic glutamate receptors. This occurred concomitantly with mitochondrial ATP hydrolysis (as evidenced by oligomycin-evoked depolarization in rotenone-treated cells); notably, no significant changes in total ATP/adenosine diphosphate levels were observed in cells exposed to Aβ, NMDA, or Aβ + NMDA for ~20 minutes, using the same protocol of single-cell analysis up to oligomycin addition (data not shown). Additionally, in cells incubated with rotenone and then exposed to NMDA, the decrease in Ca_i^{2+} levels was accompanied by a decrease in $mitCa^{2+}$ retention. In the previous studies, blockade of $mitCa^{2+}$ sequestration induced by oligomycin plus rotenone in cortical brain slices caused a reduction in Ca^{2+} influx through the NMDAR channel after glutamate treatment (Kannurpatti et al., 2000). Although this may be hypothesized for NMDA-exposed cells, an alternative rationale should be made for Aβ. In fact, although pre-exposure to rotenone inhibited Aβ-induced Ca_i^{2+} increase, mitochondria were still able to accumulate Ca^{2+}. Thus, oligomeric Aβ may not only interact with NMDARs but also interfere with mitochondria function/activity, as described previously.

Mitochondria and the ER directly communicate to maintain normal cellular homeostasis. Recently, it was shown that presenilin-1 and -2, components of the γ-secretase complex, are enriched in the MAMs (Area-Gomez et al., 2009) and that mutations in presenilin-1 and -2 upregulate MAM function and increase ER-mitochondria connectivity (Area-Gomez et al., 2012). We have previously shown in cortical neurons that $A\beta_{1-40}$, in a fibrillar state, induces the release of ER Ca^{2+} through IP_3R and RyR channels (Ferreiro et al., 2004), which is implicated in mitochondrial depolarization, release of cytochrome c, translocation of Bax to mitochondria, and apoptosis (Ferreiro et al., 2006, 2008). Our results largely suggest that the potentiation of $mitCa^{2+}$ retention that occurs in cells exposed to Aβ + NMDA is related to ER-mitochondria crosstalk. Indeed, by inhibiting IP_3R with XeC, we show decreased $mitCa^{2+}$ retention in cells exposed to Aβ + NMDA in a process involving the MCU. Interestingly, along with the inhibition of ER Ca^{2+} transfer, XeC also prevented mitochondrial depolarization occurring in response to Aβ + NMDA stimulation. Nevertheless, we cannot exclude that XeC can somehow affect NMDARs function. In fact, in cells pre-exposed to XeC and treated with Aβ + NMDA, we observed a decrease in Ca^{2+} entry to the cytosol, further preventing mitochondrial depolarization. Also, we cannot exclude the possible interactions of Aβ with metabotropic receptors leading to IP_3 formation and ER Ca^{2+} release; however, studies linking the activation of metabotropic receptors with ER stress in neuronal cells exposed to Aβ oligomers are presently missing.

Altogether, these data demonstrate that Aβ induces an immediate increase in Ca_i^{2+} and mitochondrial depolarization, partially mediated through GluN2B-containing NMDARs, highlighting the role of NMDARs in Ca^{2+} dyshomeostasis in AD. This study further evidences the intricate role of mitochondria in retaining Ca^{2+} in Aβ-treated cells. Moreover, when extracellular accumulation of Aβ occurs concomitantly with a direct activation of GluN2B-containing NMDARs by glutamate in the synaptic cleft, $mitCa^{2+}$ retention is exacerbated involving ER Ca^{2+} release through the IP_3R and the MCU (Fig. 7). These data deepen the understanding of the mechanisms underlying Aβ-induced neuronal and synapse dysfunction involving NMDARs overactivation and ER-mitochondria crosstalk; this may be exacerbated during aging and further contribute for AD neurodegeneration, emphasizing mitochondria and GluN2B subunits as therapeutic targets in early stages of AD pathogenesis.

Disclosure statement

The authors have no conflict of interest to declare.

Acknowledgements

The work was supported by Fundo Europeu de Desenvolvimento Regional (FEDER) through "Programa Operacional Factores de Competitividade (COMPETE)," "Fundação para a Ciência e a Tecnologia," project references PEst-C/SAU/LA0001/2013-2014 and PTDC/SAU-NEU/71675/2006, postdoctoral fellowships SFRH/BPD/43536/2008 and SFRH/BPD/86551/2012, *Quadro de Referência Estratégico Nacional 2007–2013* project "Desenvolvimento e Operacionalização da Investigação de Translação," Lundbeck Foundation, and the Center for Neuroscience and Cell Biology, University of Coimbra, Coimbra, Portugal.

References

Agostinho, P., Oliveira, C.R., 2003. Involvement of calcineurin in the neurotoxic effects induced by amyloid-beta and prion peptides. Eur. J. Neurosci. 17, 1189–1196.

Alberdi, E., Sánchez-Gómez, M.V., Cavaliere, F., Pérez-Samartín, A., Zugaza, J.L., Trullas, R., Domercq, M., Matute, C., 2010. Amyloid beta oligomers induce Ca^{2+} dysregulation and neuronal death through activation of ionotropic glutamate receptors. Cell Calcium 47, 264–272.

Area-Gomez, E., de Groof, A.J., Boldogh, I., Bird, T.D., Gibson, G.E., Koehler, C.M., Yu, W.H., Duff, K.E., Yaffe, M.P., Pon, L.A., Schon, E.A., 2009. Presenilins are enriched in endoplasmic reticulum membranes associated with mitochondria. Am. J. Pathol. 175, 1810–1816.

Area-Gomez, E., Del Carmen Lara Castillo, M., Tambini, M.D., Guardia-Laguarta, C., de Groof, A.J., Madra, M., Ikenouchi, J., Umeda, M., Bird, T.D., Sturley, S.L., Schon, E.A., 2012. Upregulated function of mitochondria-associated ER membranes in Alzheimer disease. EMBO J. 31, 4106–4123.

Arispe, N., Pollard, H.B., Rojas, E., 1993. Giant multilevel cation channels formed by Alzheimer disease amyloid β-protein [AβP-(1–40)] in bilayer membranes. Proc. Natl. Acad. Sci. U.S.A. 90, 10573–10577.

Bi, X., Gall, C.M., Zhou, J., Lynch, G., 2002. Uptake and pathogenic effects of amyloid beta peptide 1-42 are enhanced by integrin antagonists and blocked by NMDA receptor antagonists. Neuroscience 112, 827–840.

Caldeira, G.L., Ferreira, I.L., Rego, A.C., 2013. Impaired transcription in Alzheimer's disease: key role in mitochondrial dysfunction and oxidative stress. J. Alzheimers Dis. 34, 115–131.

Camandola, S., Mattson, M.P., 2011. Aberrant subcellular neuronal calcium regulation in aging and Alzheimer's disease. Biochim. Biophys. Acta 1813, 965–973.

Celsi, F., Pizzo, P., Brini, M., Leo, S., Fotino, C., Pinton, P., Rizzuto, R., 2009. Mitochondria, calcium and cell death: a deadly triad in neurodegeneration. Biochim. Biophys. Acta 1787, 335–344.

Costa, R.O., Lacor, P.N., Ferreira, I.L., Resende, R., Auberson, Y.P., Klein, W.L., Oliveira, C.R., Rego, A.C., Pereira, C.M., 2012. Endoplasmic reticulum stress occurs downstream of GluN2B subunit of N-methyl-d-aspartate receptor in mature hippocampal cultures treated with amyloid-β oligomers. Aging Cell 11, 823–833.

De Felice, F.G., Velasco, P.T., Lambert, M.P., Viola, K., Fernandez, S.J., Ferreira, S.T., Klein, W.L., 2007. Abeta oligomers induce neuronal oxidative stress through an N-methyl-D-aspartate receptor-dependent mechanism that is blocked by the Alzheimer drug memantine. J. Biol. Chem. 282, 11590–11601.

Deshpande, A., Kawai, H., Metherate, R., Glabe, C.G., Busciglio, J., 2009. A role for synaptic zinc in activity-dependent Abeta oligomer formation and accumulation at excitatory synapses. J. Neurosci. 29, 4004–4015.

Domingues, A., Almeida, S., da Cruz e Silva, E.F., Oliveira, C.R., Rego, A.C., 2007. Toxicity of beta-amyloid in HEK293 cells expressing NR1/NR2A or NR1/NR2B N-methyl-D-aspartate receptor subunits. Neurochem. Int. 50, 872–880.

Dragicevic, N., Mamcarz, M., Zhu, Y., Buzzeo, R., Tan, J., Arendash, G.W., Bradshaw, P.C., 2010. Mitochondrial amyloid-beta levels are associated with the extent of mitochondrial dysfunction in different brain regions and the degree of cognitive impairment in Alzheimer's transgenic mice. J. Alzheimers Dis. 20 (Suppl 2), S535–S550.

Du, H., Guo, L., Fang, F., Chen, D., Sosunov, A.A., McKhann, G.M., Yan, Y., Wang, C., Zhang, H., Molkentin, J.D., Gunn-Moore, F.J., Vonsattel, J.P., Arancio, O., Chen, J.X., Yan, S.D., 2008. Cyclophilin D deficiency attenuates mitochondrial and neuronal perturbation and ameliorates learning and memory in Alzheimer's disease. Nat. Med. 14, 1097–1105.

Du, H., Guo, L., Yan, S.S., 2012. Synaptic mitochondrial pathology in Alzheimer's disease. Antioxid. Redox Signal. 16, 1467–1475.

Du, H., Guo, L., Yan, S., Sosunov, A.A., McKhann, G.M., Yan, S.S., 2010. Early deficits in synaptic mitochondria in an Alzheimer's disease mouse model. Proc. Natl. Acad. Sci. U. S. A. 107, 18670–18675.

Ferreira, I.L., Bajouco, L.M., Mota, S.I., Auberson, Y.P., Oliveira, C.R., Rego, A.C., 2012. Amyloid beta peptide 1-42 disturbs intracellular calcium homeostasis through activation of GluN2B-containing N-methyl-D-aspartate receptors in cortical cultures. Cell Calcium 51, 95–106.

Ferreira, I.L., Resende, R., Ferreiro, E., Rego, A.C., Pereira, C.F., 2010. Multiple defects in energy metabolism in Alzheimer's disease. Curr. Drug Targets 11, 1193–1206.

Ferreiro, E., Baldeiras, I., Ferreira, I.L., Costa, R.O., Rego, A.C., Pereira, C.F., Oliveira, C.R., 2012. Mitochondrial- and endoplasmic reticulum-associated oxidative stress in Alzheimer's disease: from pathogenesis to biomarkers. Int. J. Cell Biol. 2012, 735206.

Ferreiro, E., Oliveira, C.R., Pereira, C., 2004. Involvement of endoplasmic reticulum Ca^{2+} release through ryanodine and inositol 1,4,5-triphosphate receptors in the neurotoxic effects induced by the amyloid-beta peptide. J. Neurosci. Res. 76, 872–880.

Ferreiro, E., Oliveira, C.R., Pereira, C.M., 2008. The release of calcium from the endoplasmic reticulum induced by amyloid-beta and prion peptides activates the mitochondrial apoptotic pathway. Neurobiol. Dis. 30, 331–342.

Ferreiro, E., Resende, R., Costa, R., Oliveira, C.R., Pereira, C.M., 2006. An endoplasmic-reticulum-specific apoptotic pathway is involved in prion and amyloid-beta peptides neurotoxicity. Neurobiol. Dis. 23, 669–678.

Gibson, G.E., Peterson, C., 1987. Calcium and the aging nervous system. Neurobiol. Aging 8, 329–343.

Gouras, G.K., Tsai, J., Naslund, J., Vincent, B., Edgar, M., Checler, F., Greenfield, J.P., Haroutunian, V., Buxbaum, J.D., Xu, H., Greengard, P., Relkin, N.R., 2000. Intraneuronal Abeta42 accumulation in human brain. Am. J. Pathol. 156, 15–20.

Guo, L., Du, H., Yan, S., Wu, X., McKhann, G.M., Chen, J.X., Yan, S.S., 2013. Cyclophilin D deficiency rescues axonal mitochondrial transport in Alzheimer's neurons. PLoS One 8, e54914.

Haass, C., Selkoe, D.J., 2007. Soluble protein oligomers in neurodegeneration: lessons from the Alzheimer's amyloid beta-peptide. Nat. Rev. Mol. Cell Biol. 8, 101–112.

Hansson Petersen, C.A., Alikhani, N., Behbahani, H., Wiehager, B., Pavlov, P.F., Alafuzoff, I., Leinonen, V., Ito, A., Winblad, B., Glaser, E., Ankarcrona, M., 2008. The amyloid beta-peptide is imported into mitochondria via the TOM import machinery and localized to mitochondrial cristae. Proc. Natl. Acad. Sci. U. S. A. 105, 13145–13150.

Hauptmann, S., Scherping, I., Dröse, S., Brandt, U., Schulz, K.L., Jendrach, M., Leuner, K., Eckert, A., Müller, W.E., 2009. Mitochondrial dysfunction: an early event in Alzheimer pathology accumulates with age in AD transgenic mice. Neurobiol. Aging 30, 1574–1586.

Kannurpatti, S.S., Joshi, P.G., Joshi, N.B., 2000. Calcium sequestering ability of mitochondria modulates influx of calcium through glutamate receptor channel. Neurochem. Res. 25, 1527–1536.

Klein, W.L., 2006. Synaptic targeting by Abeta oligomers (ADDLS) as a basis for memory loss in early Alzheimer's disease. Alzheimers Dement. 2, 43–55.

Kutsuwada, T., Sakimura, K., Manabe, T., Takayama, C., Katakura, N., Kushiya, E., Natsume, R., Watanabe, M., Inoue, Y., Yagi, T., Aizawa, S., Arakawa, M., Takahashi, T., Nakamura, Y., Mori, H., Mishina, M., 1996. Impairment of suckling response, trigeminal neuronal pattern formation, and hippocampal LTD in NMDA receptor epsilon 2 subunit mutant mice. Neuron 16, 333–344.

Lazarov, O., Lee, M., Peterson, D.A., Sisodia, S.S., 2002. Evidence that synaptically released beta-amyloid accumulates as extracellular deposits in the hippocampus of transgenic mice. J. Neurosci. 22, 9785–9793.

Malinow, R., 2012. New developments on the role of NMDA receptors in Alzheimer's disease. Curr. Opin. Neurobiol. 22, 559–563.

Matos, M., Augusto, E., Oliveira, C.R., Agostinho, P., 2008. Amyloid-beta peptide decreases glutamate uptake in cultured astrocytes: involvement of oxidative stress and mitogen-activated protein kinase cascades. Neuroscience 156, 898–910.

Mattson, M.P., Partin, J., Begley, J.G., 1998. Amyloid beta-peptide induces apoptosis-related events in synapses and dendrites. Brain Res. 807, 167–176.

Moreira, P.I., Santos, M.S., Moreno, A., Oliveira, C., 2001. Amyloid β-peptide promotes permeability transition pore in brain mitochondria. Biosci. Rep. 2, 789–800.

Mota, S.I., Ferreira, I.L., Pereira, C., Oliveira, C.R., Rego, A.C., 2012. Amyloid-beta peptide 1-42 causes microtubule deregulation through N-methyl-D-aspartate receptors in mature hippocampal cultures. Curr. Alzheimer Res. 9, 844–856.

Mota, S.I., Ferreira, I.L., Rego, A.C., 2014. Dysfunctional synapse in Alzheimer's disease - a focus on NMDA receptors. Neuropharmacology 76 (Pt A), 16–26.

Nicholls, D.G., 2009. Mitochondrial calcium function and dysfunction in the central nervous system. Biochim. Biophys. Acta 1787, 1416–1424.

Oliveira, J.M., Chen, S., Almeida, S., Riley, R., Gonçalves, J., Oliveira, C.R., Hayden, M.R., Nicholls, D.G., Ellerby, L.M., Rego, A.C., 2006. Mitochondrial-dependent Ca^{2+} handling in Huntington's disease striatal cells: effect of histone deacetylase inhibitors. J. Neurosci. 26, 11174–11186.

Pagani, L., Eckert, A., 2011. Amyloid-Beta interaction with mitochondria. Int. J. Alzheimers Dis. 2011, 925050.

Papouin, T., Ladépêche, L., Ruel, J., Sacchi, S., Labasque, M., Hanini, M., Groc, L., Pollegioni, L., Mothet, J.P., Oliet, S.H., 2012. Synaptic and extrasynaptic NMDA receptors are gated by different endogenous coagonists. Cell 150, 633–646.

Parameshwaran, K., Dhanasekaran, M., Suppiramaniam, V., 2008. Amyloid beta peptides and glutamatergic synaptic dysregulation. Exp. Neurol. 210, 7–13.

Rego, A.C., Ward, M.W., Nicholls, D.G., 2001. Mitochondria control ampa/kainate receptor-induced cytoplasmic calcium deregulation in rat cerebellar granule cells. J. Neurosci. 21, 1893–1901.

Resende, R., Ferreiro, E., Pereira, C., Oliveira, C.R., 2008. Neurotoxic effect of oligomeric and fibrillar species of amyloid-beta peptide 1-42: involvement of

endoplasmic reticulum calcium release in oligomer-induced cell death. Neuroscience 155, 725–737.
Sanz-Blasco, S., Valero, R.A., Rodríguez-Crespo, I., Villalobos, C., Núñez, L., 2008. Mitochondrial Ca^{2+} overload underlies Abeta oligomers neurotoxicity providing an unexpected mechanism of neuroprotection by NSAIDs. PLoS One 3, e2718.
Stanika, R.I., Villanueva, I., Kazanina, G., Andrews, S.B., Pivovarova, N.B., 2012. Comparative impact of voltage-gated calcium channels and NMDA receptors on mitochondria-mediated neuronal injury. J. Neurosci. 32, 6642–6650.
Supnet, C., Bezprozvanny, I., 2010. The dysregulation of intracellular calcium in Alzheimer disease. Cell Calcium 47, 183–189.
Texidó, L., Martín-Satué, M., Alberdi, E., Solsona, C., Matute, C., 2011. Amyloid β peptide oligomers directly activate NMDA receptors. Cell Calcium 49, 184–190.
Tovar, K.R., Sprouffske, K., Westbrook, G.L., 2000. Fast NMDA receptor-mediated synaptic currents in neurons from mice lacking the epsilon2 (NR2B) subunit. J. Neurophysiol. 83, 616–620.
Ward, M.W., Rego, A.C., Frenguelli, B.G., Nicholls, D.G., 2000. Mitochondrial membrane potential and glutamate excitotoxicity in cultured cerebellar granule cells. J. Neurosci. 20, 7208–7219.